

# PHYSICS-INFORMED RADIAL BASIS FUNCTION NETWORKS AND KOLMOGOROV-ARNOLD NETWORKS

**Anonymous authors**

Paper under double-blind review

## ABSTRACT

Physics-informed neural networks are trained by minimizing the loss function, which is the sum of the squares of the residuals of the equation or system of equations being solved. Such networks do not require grid construction, which is especially important when solving inverse boundary value problems and problems with a complex solution domain. We use radial basis function networks with a Gaussian function. Physics-informed radial basis function networks are easier to train than fully connected networks. They allow one to analytically obtain formulas for the gradient of the loss function. A special feature of our approach to training networks based on radial basis functions is the adjustment of not only the weights, but also the parameters of the radial basis functions, which does not require the selection of parameters of the radial basis functions and accelerates the training process. Algorithms for solving direct and inverse boundary value problems, an algorithm for solving a system of differential equations for modeling the Kovasznay flow have been developed. Programs have been developed that use various algorithms for training physics-informed radial basis function networks.

## 1 INTRODUCTION

Neural networks are applicable for solving boundary value problems described by partial differential equations (1; 2). This possibility is based, first of all, on the fact that neural networks are universal function approximators. Cybenko's theorem states that an artificial neural network with one hidden layer can approximate any continuous function of many variables with any accuracy (3). Hornik (4) proved that a multilayer perceptron with an arbitrary number of hidden layers and an arbitrary number of neurons in each layer can approximate any continuous function with any accuracy on a compact set. It was also proved that such approximation is possible for arbitrary activation functions if they are bounded, continuous, non-polynomial and non-constant. A variational approach is also used to solve partial differential equations on neural networks: the solution to the problem is found by minimizing the error functional of the neural network. The residuals of the approximate solution obtained by the network at a certain set of trial points inside, on the boundary of the solution domain and, possibly, at points with additional conditions are used as the error functional. Estimating the norm of this residual gives a better interpretable estimate of the accuracy of the problem solution than estimates of the accuracy of the solution of grid methods, for which only the order of accuracy of the approximation and the remainder of the solution of the system of grid equations are known. Trial points are usually located randomly in the solution domain. Currently, a specific class of neural networks has been formed for solving partial differential equations on neural networks - physics-informed neural networks. Physics-informed neural networks (5; 6; 7) include in the network structure a mathematical model of some physical phenomenon, for example, partial differential equations. When solving direct problems, PINN do not require examples with known values for training. Such networks solve the problem of low data availability in many scientific and engineering problems where traditional machine learning methods are ineffective. Additional conditions can also be used, for example, when solving inverse problems, experimental information about the solution at individual points of the region is used. In physics-informed neural networks, the mathematical model is a regulating factor that improves the quality of the solution. Radial basis function networks are successfully used to solve partial differential equations. Radial basis function

networks (8; 2; 9) are simpler than fully connected networks, since they contain only two layers - a layer of radial basis functions (10) and a linear layer. The simplicity of the network architecture simplifies the training of radial basis function networks, for example, it allows analytical calculation of the gradients of the error functional. The authors have developed second-order gradient learning algorithms for radial basis function networks, in which not only the network weights are configured, but also the parameters of the radial basis functions. The efficiency of the developed algorithms has been demonstrated by solving direct (11; 12) and inverse (13; 14) boundary value problems. Physically informed radial basis function networks (15; 14; 16; 17) are an effective tool for solving partial differential equations. Radial basis function networks have some similarities with Kolmogorov-Arnold networks. Kolmogorov-Arnold networks are based on the Kolmogorov-Arnold theorem (18), which states that any continuous multivariate function  $f(x_1, x_2, \dots, x_d)$  defined on a bounded domain can be represented as a finite composition of continuous one-dimensional functions and addition operations. Mathematically, this is expressed as:

$$f(x_1, x_2, \dots, x_d) = \sum_{q=1}^{2d+1} \Phi_q \left( \sum_{p=1}^d \psi_{q,p}(x_p) \right),$$

where:  $\Phi_q$  and  $\psi_{q,p}$  are continuous one-dimensional functions. In (19), R. Hecht-Nielsen proposed a neural network that directly reflects the Kolmogorov-Arnold representation, where the hidden  $d$  layer computes the internal sums  $\sum_{p=1}^d \psi_{q,p}(x_p)$  and the output layer computes the external sums  $\sum_{q=1}^{2d+1} \Phi_q(\cdot)$ . But R. Hecht-Nielsen did not propose methods for finding the specific functions  $\Phi_q$  and  $\psi_{q,p}$ , which makes his network difficult to implement directly. Therefore, such networks have not been developed.

Kolmogorov-Arnold networks (20) are also based on the Kolmogorov-Arnold theorem and introduce significant innovations in architecture and training. Unlike the Hecht-Nielsen approach, Kolmogorov-Arnold networks replace fixed activation functions with trainable cubic basis splines (B-splines) in which the basis function weights are adjustable. Other basis functions can also be used.

Radial basis function networks are similar to Kolmogorov-Arnold networks in that in both types of networks, the inputs of the first layer are nonlinearly transformed using basis functions and added together. In physics-informed radial basis function networks implementing the regression problem, the second nonlinear layer is absent. In the one-dimensional case, as shown in (21), a complete analogy between Kolmogorov-Arnold networks and radial basis function networks can be traced. In the multidimensional case, there is no analogy, since the basis functions are functions of many variables, which violates the conditions of the Kolmogorov-Arnold theorem. There are no data comparing radial basis function networks and Kolmogorov-Arnold networks. Solving partial differential equations on physics-informed neural networks is a neural network approximation of the problem solution. It is easier to approximate a multidimensional result function with multidimensional functions than with one-dimensional ones, so it can be assumed that with an increase in the problem dimension and in the case of inhomogeneous media, radial basis function networks will outperform Kolmogorov-Arnold networks. To enhance the positive qualities of radial basis function networks, it is necessary to adapt radial basis functions to the specific features of the problem being solved, which requires adjusting not only the network weights, but also the parameters of the radial basis functions. Such adjustment is implemented in the radial basis function network training algorithms we propose.

The aim of this work is to develop algorithms for solving various boundary value problems on networks of radial basis functions trained by gradient algorithms with the adjustment of not only the network weights, but also the parameters of the radial basis functions.

## 2 DEVELOPMENT OF ALGORITHMS FOR LEARNING PHYSICS-INFORMED RADIAL BASIS FUNCTION NETWORKS

The output of the radial basis function network is described by the expression

108

109

110

111

$$v(x, y) = \sum_{k=1}^{n_{RBF}} \omega_k \varphi_k(x, y),$$

112

where  $n_{RBF}$  — number of radial basis functions (or number of neurons),  $\omega_k$  — weight of the  $k$  th neuron,  $\varphi_k(x, y)$  — value of the  $k$  th radial basis function at point  $x$ .

114

To solve the problems in this article, Gauss functions were used as radial basis functions, which have the form

116

117

$$\varphi_k(x, y) = e^{-\frac{(x-c_{k1})^2+(y-c_{k2})^2}{2a_k^2}}$$

118

where  $c_{k1}$  and  $c_{k2}$  — centers of functions,  $a_k$  — width of functions.

119

Consider a model direct problem in operator form having the form

120

121

$$Lu(\mathbf{x}) = f(\mathbf{x}), x \in \Omega,$$

122

123

$$Bu(\mathbf{x}) = p(\mathbf{x}), x \in \partial\Omega,$$

124

where  $u$  — desired solution;  $L$  — differential operator; operator  $B$  sets the boundary conditions;  $\Omega$  — solution area;  $\partial\Omega$  — regional boundary;  $f$  and  $p$  — known functions.

126

Let us consider the effectiveness of the Levenberg-Marquardt diagonal method for solving the Poisson equation

128

129

$$\frac{\partial^2 u}{\partial x^2} + \frac{\partial^2 u}{\partial y^2} = f(x, y), (x, y) \in \Omega,$$

130

131

$$u(x, y) = p(x, y), (x, y) \in \partial\Omega,$$

132

where  $\Omega$  — estimated area;  $\partial\Omega$  — the boundary of the computational domain;  $f = \sin(\pi x) \cdot \sin(\pi y)$ ,  $p = 0$ .

134

The error function can be written as

135

136

137

138

$$\frac{1}{2} \sum_{i=1}^N \left( \frac{\partial^2 u_i}{\partial x^2} + \frac{\partial^2 u_i}{\partial y^2} - f_i \right)^2 + \frac{\lambda}{2} \sum_{j=1}^K (u_j - p_j)^2$$

139

where  $N$  – number of internal test points,  $K$  – number of boundary test points,  $\lambda$  – penalty multiplier.

140

141

142

143

144

145

146

147

148

The network was trained to solve the Poisson equation using various methods: gradient descent, Nesterov, Levenberg-Marquardt, and diagonal approximation of the Hessian. The gradient method converges at a linear rate. And Newton's method has a quadratic convergence rate. But to implement Newton's method, it is necessary to find the Hessian, the inverse Hessian matrix, and solve the system. These are quite labor-intensive tasks. Especially finding the inverse matrix. Therefore, some modification can be considered. We will consider the Hessian to be a diagonal matrix. We equate all mixed partial derivatives to zero. Thanks to this, we can easily find the inverse matrix. We can also adjust the convergence rate of the algorithm. this will help to circumvent the problem of linear minimization of the error functional when the second derivatives become close to zero.

149

150

151

152

Due to the convenient structure of neural networks, the formulas of the second derivatives for the Poisson equation were obtained analytically. The values of the elements located on the main diagonal of the Hessian for this problem can be obtained based on the following formula

153

154

155

156

157

158

159

160

161

$$\frac{\partial^2 I}{\partial \omega_k^2} = \sum_{i=1}^N \left( e^{-\frac{(x_i-c_{k1})^2+(y_i-c_{k2})^2}{2a_k^2}} \left( \frac{(x_i-c_{k1})^2 + (y_i-c_{k2})^2 - 2a_k^2}{a_k^4} \right)^2 + \lambda \sum_{j=1}^K \left( e^{-\frac{(x_i-c_{k1})^2+(y_i-c_{k2})^2}{2a_k^2}} \right)^2 \right)$$

where  $c_{k1}$  and  $c_{k2}$  — centers of functions,  $a_k$  — width of functions.

The vector of weight coefficients in the Hessian diagonal approximation method is calculated using the formula

162  
163  
164  
165  
166  
167  
168  
169  
170  
171  
172  
173  
174  
175  
176  
177  
178  
179  
180  
181  
182  
183  
184  
185  
186  
187  
188  
189  
190  
191  
192  
193  
194  
195  
196  
197  
198  
199  
200  
201  
202  
203  
204  
205  
206  
207  
208  
209  
210  
211  
212  
213  
214  
215

$$\omega_i^{k+1} = \omega_i^k - \eta \left( \frac{\partial^2 I^k}{\partial \omega_i^{k2}} + \mu \right)^{-1} \frac{\partial I^k}{\partial \omega_i^k}$$

where  $\frac{\partial I^k}{\partial \omega_i^k}$  — gradient vector components,  $\eta$  and  $\mu$  — selected coefficients.

The Hessian diagonal approximation method achieved an accuracy of  $10^{-3}$  in an average of 250 iterations. The gradient descent method did not achieve an accuracy of  $10^{-3}$ . The Nesterov method achieved an accuracy of  $10^{-3}$  in an average of 500 iterations.

Let us consider the efficiency of the modified Levenberg-Marquardt method with the adjustment of the parameters of radial basis functions for solving new model problems describing processes in a piecewise homogeneous medium.

The model problem describing processes in a piecewise homogeneous medium is presented in the form of the following equation

$$\frac{\partial}{\partial x} (\sigma_i(x, y) \frac{\partial u}{\partial x}) + \frac{\partial}{\partial y} (\sigma_i(x, y) \frac{\partial u}{\partial y}) = f(x, y),$$

$$(x, y) \in \Omega, i = 1, 2,$$

$$u(x, y) = p(x, y), (x, y) \in \partial\Omega,$$

where  $\Omega$  — estimated area;  $\partial\Omega$  — the boundary of the computational domain;  $f = \sin(2\pi x) \cdot \sin(\pi y)$ ,  $p = 0$ ,  $\sigma_i$  — a function describing the properties of the environment. The solution area is a square with unit side length, divided at  $x = 0, 5$  by a vertical line into two subareas with different values of  $\sigma_i$ ,  $i = 1, 2$ .  $x \in [0; 1]$ ,  $y \in [0; 1]$ .

The problem is decomposed into two problems for regions 1 and 2 taking into account the conjugation conditions.

For area 1:

$$\frac{\partial}{\partial x} (\sigma_1(x, y) \frac{\partial u_1}{\partial x}) + \frac{\partial}{\partial y} (\sigma_1(x, y) \frac{\partial u_1}{\partial y}) = f_1(x, y),$$

$$(x, y) \in \Omega, i = 1, 2,$$

$$u_1(x, y) = p_1(x, y), (x, y) \in \partial\Omega_1,$$

where  $\Omega_1$  — design area 1;  $\partial\Omega_1$  — design area boundary 1.

For area 2:

$$\frac{\partial}{\partial x} (\sigma_2(x, y) \frac{\partial u_2}{\partial x}) + \frac{\partial}{\partial y} (\sigma_2(x, y) \frac{\partial u_2}{\partial y}) = f_2(x, y),$$

$$(x, y) \in \Omega, i = 1, 2,$$

$$u_2(x, y) = p_2(x, y), (x, y) \in \partial\Omega_2,$$

where  $\Omega_2$  — design domain 2;  $\partial\Omega_2$  — design area boundary 2.

At the interface between the media, the interface conditions must be fulfilled.

$$u_1 |_{S=} u_2 |_{S}, \sigma_1 \frac{\partial u_1}{\partial x} |_{S=} \sigma_2 \frac{\partial u_2}{\partial x} |_{S}$$

where  $S$  - regional boundary.

The radial basis functions were Gaussian functions. As a result of training, not only the vector of weights, but also the parameters of radial basis functions were tuned, since it is important to tune all parameters of the radial basis function network. The Levenberg-Marquardt algorithm is used to train the radial basis function network (22). The Levenberg-Marquardt method is equivalent to the fast confidence region method (23), but does not require solving the conditional optimization problem at each training iteration. The single vector of weights and parameters of the radial basis function network at iteration  $k$  is found by the formula  $\theta^{k+1} = \theta^k + \Delta\theta^{k+1}$ , in which the vector of correction parameters  $\theta^k$  is found from the solution of the system of linear algebraic equations

216  
217  
218  
219  
220  
221  
222  
223  
224  
225  
226  
227  
228  
229  
230  
231  
232  
233  
234  
235  
236  
237  
238  
239  
240  
241  
242  
243  
244  
245  
246  
247  
248  
249  
250  
251  
252  
253  
254  
255  
256  
257  
258  
259  
260  
261  
262  
263  
264  
265  
266  
267  
268  
269

$$(\mathbf{J}_{k-1}^T \mathbf{J}_{k-1} + \mu_k \mathbf{E}) \Delta \theta^k = -\mathbf{g}_{k-1},$$

where  $\mathbf{J}_{k-1}$  and  $\mathbf{J}_k$  — Jacobi matrices calculated in  $k-1$  and  $k$  iterations,  $\mathbf{E}$  — unit matrix,  $\mu_k$  — regularization parameter changing at each training step,  $\mathbf{g} = \mathbf{J}^T r$  — is the gradient vector of the loss function along the parameter vector  $\theta$ ,  $r$  — vector of unconstraints in internal and boundary trial points.

Two radial basis function networks are used for the solution, since each of the networks describes its own area. During network initialization, the centers of radial basis functions were located on a uniform grid. The vectors of weights and widths were initialized with random values close to zero. Currently, there are no theoretical estimates of the optimal number of neurons and test points. The authors' experimental studies have shown that there is an optimal number of neurons and test points for each task. With a small number of neurons and test points, low decision accuracy is obtained or the learning process does not converge. With a large number of neurons and test points, high accuracy of the solution is ensured, but the network operation time to obtain a solution increases significantly. The number of neurons, test points and initial values of the parameters of the radial basis functions were selected experimentally. As a result of the experiments, the following values were obtained. The number of neurons used to solve a direct boundary value problem for each of the two regions is 64. The initial values of the components of the width vector are 0.2. The number of internal test points for two regions is  $N=80$ . The number of boundary test points for two regions is  $K=80$ . The number of test points on the median line is 20. The coordinates of the collocation points were generated as random numbers evenly distributed in the solution area.

Iterations were performed until the average square error was reached, equal to  $10^{-10}$ . The radial basis function network was trained by the Levenberg-Marquardt method. The solution is achieved in an average of 570 iterations. Due to the random initialization of the network, the number of iterations varies in different experiments.

The inverse boundary value problem is described by a partial differential equation

$$\frac{\partial}{\partial x} (k(\mathbf{x}) \frac{\partial u}{\partial x}) + \frac{\partial}{\partial y} (k(\mathbf{x}) \frac{\partial u}{\partial y}) = f(\mathbf{x}), \mathbf{x} \in \Omega,$$

where  $k(\mathbf{x})$  — continuous unknown function describing the environment,  $\mathbf{x}$  — the coordinate vector,  $\Omega$ - solution area. Without knowing the position of the interface boundary, it is impossible to model a piecewise homogeneous function of the medium. Therefore, when solving the inverse problem, the piecewise homogeneous function describing the medium was approximately replaced by a continuous function. The boundary conditions have the form

$$Bu(\mathbf{x}) = p(\mathbf{x}), x \in \partial\Omega,$$

where  $\partial\Omega$  — the border of the region. It is necessary to find the solution  $u$  and the  $k(\mathbf{x})$  function by the solution known in some set of points

$$u(\mathbf{z}) = \psi(\mathbf{z}), \mathbf{z} \in Z, Z \subset \Omega$$

moreover,  $\psi(\mathbf{z})$  in real problems is the result of measurement with some error. The solution is made on radial basis function networks. To obtain the values of additional conditions, a direct problem has been solved previously on a radial basis function network. The direct boundary value problem was a differential equation for a piecewise homogeneous medium with coefficients equal to 2 and 5.5. We use parametric optimization (24). To do this, we approximate the unknown  $k(\mathbf{x})$  function with a radial basis function network

$$k_{RBF}(\mathbf{x}) = \sum_{m=1}^{M_k} \omega_m^k \varphi_m^k(\mathbf{x}; \mathbf{p}_m^k),$$

where  $M_k$  the number of radial basis functions (or the number of neurons),  $\mathbf{p}_m^u$  — weights and vectors of parameters of radial basis functions  $\varphi_m^u$ .

The solution of the  $u$  direct problem, in which the  $k(\mathbf{x})$  function is approximated by the network, is found by the second network of radial basis functions

$$u_{RBF}(\mathbf{x}) = \sum_{m=1}^{M_u} \omega_m^u \varphi_m^u(\mathbf{x}; \mathbf{p}_m^u),$$

where  $M_u$  the number of radial basis functions (or the number of neurons),  $\mathbf{p}_m^u$  — weights and vectors of parameters of radial basis functions  $\varphi_m^u$ .

Two networks were used to solve the inverse problem. The network  $k_{RBF}$  for approximating the desired function of the medium. And the network  $u_{RBF}$  to approximate the solution. The error functional was the sum of the squares of the residuals of the approximate solution at the test points inside, at the boundary of the solution domain and at the points of additional conditions.

For an incorrect inverse problem, regularization was required. The method of iterative regularization was the Morozov condition (25). The network has been trained so far

$$\sum_{m=1}^S [u(\mathbf{x}_m) - \psi(\mathbf{x}_m)]^2 > S\delta^2,$$

where  $\delta$  — the absolute error of measuring the solution at the points of additional conditions.

Gaussian functions were used as radial basis functions. The number of neurons, test points and hyperparameters of learning were selected experimentally. For both problems, the number of radial basis functions is 64. For both networks, 80 test points were used inside the solution area. For the  $u_{RBF}$  network, there are 80 test points on the boundary and 40 additional condition points. The initial values of the components of the width vector for the two regions are 0.3. All penalty coefficients of the error functional are 100. To check the efficiency of the algorithm, a problem was considered that has an absolute error of measuring the solution at the points of additional conditions equal to 0.0001. To solve this problem, the Morozov condition was used. The error functional value of  $10^{-5}$  is achieved in an average of 290 iterations.

In Fig. 1 the desired function of the medium is presented, obtained as a result of solving the inverse boundary value problem, which models processes in a piecewise homogeneous medium.

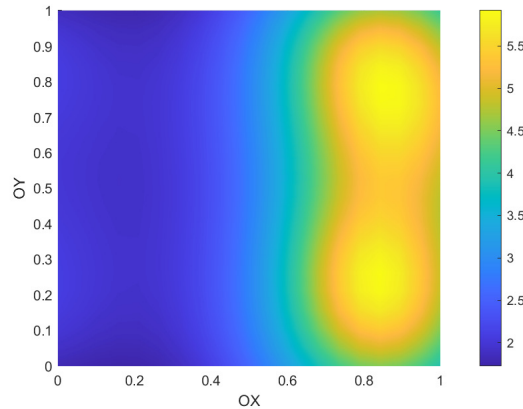


Figure 1: The environment function obtained as a result of solving the inverse boundary value problem

Judging by the graph, the neural network has successfully restored an unknown function of the medium in the process of solving the inverse boundary value problem.

The solution of the problems is implemented in the MATLAB system, which provides ease of programming and experimentation with the program and powerful graphical means of presenting the results of the solution. A feature of the implementation is the analytical calculation of the gradients of the loss function according to the parameters of the network and the Jacobi matrix, which is not difficult to implement due to the simplicity of the network structure.

### 3 MODELING A HYDRODYNAMIC PROBLEM ON PHYSICS-INFORMED RADIAL BASIS FUNCTION NETWORKS

We will demonstrate the effectiveness of physics-informed radial basis function networks for solving a model problem of hydrodynamics. For clarity, we can consider the Kovazhny current (26), since it has an analytical solution.

$$u(x, y) = -e^{(-\lambda x)} \cos(2\pi y),$$

$$v(x, y) = -\frac{\lambda}{2\pi} e^{(-\lambda x)} \sin(2\pi y),$$

$$p(x, y) = -\frac{1}{2} e^{(-2\lambda x)},$$

where parameter  $\lambda$  is defined by the following expression

$$\lambda = \sqrt{\frac{Re^2}{4} + 4\pi^2} - \frac{Re}{2},$$

where  $Re$  – Reynolds number.

The Kovaszny flow is a two-dimensional stationary flow. This problem is described by the Navier-Stokes system of equations. Two-dimensional stationary Navier-Stokes equations for an incompressible medium have the form:

$$\frac{\partial u}{\partial x} + \frac{\partial v}{\partial y} = 0, (x, y) \in \Omega,$$

$$u \frac{\partial u}{\partial x} + v \frac{\partial u}{\partial y} = -\frac{\partial p}{\partial x} + \frac{1}{Re} \left( \frac{\partial^2 u}{\partial x^2} + \frac{\partial^2 u}{\partial y^2} \right), (x, y) \in \Omega,$$

$$u \frac{\partial v}{\partial x} + v \frac{\partial v}{\partial y} = -\frac{\partial p}{\partial y} + \frac{1}{Re} \left( \frac{\partial^2 v}{\partial x^2} + \frac{\partial^2 v}{\partial y^2} \right), (x, y) \in \Omega,$$

where  $\Omega$  — is the calculated area,  $u$  – first velocity component,  $v$  – second velocity component,  $p$  – pressure. Dirichlet conditions are set at the boundary of the region.

The Kovaszny flow is the movement of the flow through the lattice. Kovaszny flow does not have an initial condition. If the flow is stationary, then the streamlines coincide with the trajectories of the particles. Since the current does not depend on time, the current lines remain unchanged. It also makes it easier to visualize the process. If the flow is unsteady, then the trajectories of the particles and the streamlines are different.

If the liquid is incompressible, then

$$\rho = const,$$

where  $\rho$  — the density of the liquid.

If the movement is stationary (27), then

$$\frac{\partial V}{\partial t} = 0.$$

For this model problem, the solution area is a square with dimensions  $x \in [0; 1]$ ,  $y \in [0; 1]$ .

The structure of neural networks allows us to calculate analytically the gradient of the error functional. This problem was solved in two ways: with analytical calculation of the gradient of the error functional and with the use of automatic differentiation. Analytical calculation allowed to speed up the work of the program. This article presents the results of the solution obtained using the analytical calculation of the gradient of the error functional. Each variable had its own network of radial basis functions based on physics. All three networks are connected by a common root-mean-square

error functionality. The functional consists of the sum of the squares of the residuals. To simplify the expression, the multiplier  $\frac{1}{2}$  has been added for the gradient of the functional. The network was trained to the value of the total error functional equal to  $10^{-4}$ . The error function can be written as

$$\begin{aligned}
 I = & \frac{1}{2} \sum_{i=1}^N \left( u_i \frac{\partial u_i}{\partial x} + v_i \frac{\partial u_i}{\partial y} + \frac{\partial p_i}{\partial x} - \frac{1}{Re} \left( \frac{\partial^2 u_i}{\partial x^2} + \frac{\partial^2 u_i}{\partial y^2} \right) \right)^2 + \\
 & \frac{1}{2} \sum_{i=1}^N \left( u_i \frac{\partial v_i}{\partial x} + v_i \frac{\partial v_i}{\partial y} + \frac{\partial p_i}{\partial y} - \frac{1}{Re} \left( \frac{\partial^2 v_i}{\partial x^2} + \frac{\partial^2 v_i}{\partial y^2} \right) \right)^2 + \\
 & \frac{1}{2} \sum_{i=1}^N \left( \frac{\partial u_i}{\partial x} + \frac{\partial v_i}{\partial y} \right)^2 + \frac{\lambda}{2} \sum_{j=1}^K (u_j - u_j^A)^2 \\
 & + \frac{\lambda}{2} \sum_{j=1}^K (v_j - v_j^A)^2 + \frac{\lambda}{2} \sum_{j=1}^K (p_j - p_j^A)^2
 \end{aligned}$$

where  $Re$  – Reynolds number,  $N$  – number of internal test points,  $K$  – number of boundary test points,  $\lambda$  – penalty multiplier,  $u_j^A, v_j^A, p_j^A$  – analytical value of the  $j$ th test point at the boundary of the region.

The model is implemented in the MATLAB environment. The centers of the radial basis functions of each network were located on a uniform grid. The weight and width vectors were initialized with zero values. Experiments were conducted for each network to select the optimal number of neurons and trial points. The number of neurons for each physics-informed radial basis function networks is 64. The number of interior trial points for each network is 100. The number of boundary trial points for each network is 40. The coordinates of collocation points were generated as random numbers that were uniformly distributed in the solution domain. The network was trained using Nesterov's method. Only the weights were customizable. The value of the error functional equal to  $10^{-2}$  is achieved in 15 iterations on average. The location of the test points is shown in Figure 2.

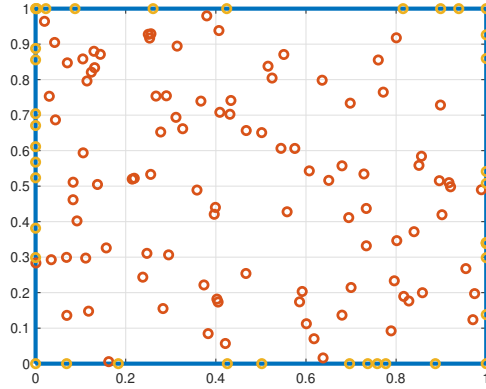


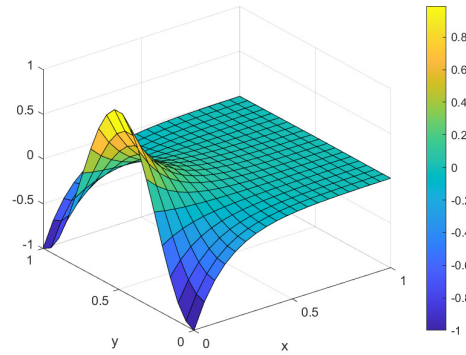
Figure 2: Test points

Let us analyze the effectiveness of the Nesterov method using the example of a model problem simulating the Kovazhny flow. The Nesterov method uses the history of parameter changes and the idea of the pulse accumulation method (28; 22). The formula for calculating the parameters in this case takes the form

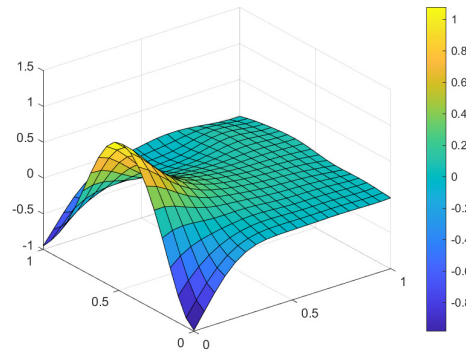
$$\Delta\Theta^{(k+1)} = \alpha\Delta\Theta^{(k)} - \gamma\text{grad}I(\Theta^{(k)}) - \alpha\Delta\Theta^{(k)}.$$

where  $\Theta$  — the vector of one of the network parameters (we can consider the vector of all parameters),  $\gamma$  — the selected numerical coefficient (learning rate),  $\alpha$  — the moment coefficient, which takes values in the interval  $[-0.5; 1.5]$ .

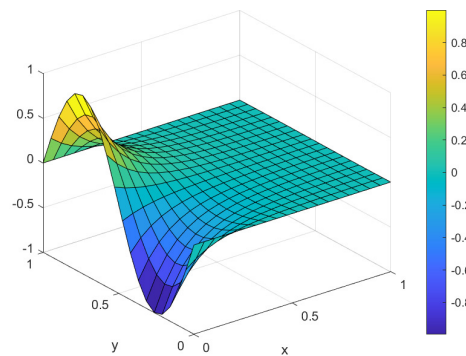
432 Plots of analytical solutions for velocity and pressure components are presented in Figures 3, 5, 7.  
 433 The graphs obtained as a result of the network operation are shown in Figures 4, 6, 8. They have  
 434 a visual similarity to the analytical solution. The MSE for the first component of the velocity is on  
 435 average  $10^{-6}$ . The MSE for the second component of the velocity is on average  $10^{-6}$ . The MSE for  
 436 pressure averages  $10^{-4}$ . This is a testament to the effectiveness of the program.  
 437  
 438  
 439  
 440  
 441  
 442  
 443  
 444  
 445  
 446  
 447  
 448  
 449  
 450



451 Figure 3: Analytical solution for the first velocity component  
 452



453  
 454  
 455  
 456  
 457  
 458  
 459  
 460  
 461  
 462  
 463  
 464  
 465  
 466  
 467  
 468 Figure 4: The first component of speed resulting from network operation  
 469



470  
 471  
 472  
 473  
 474  
 475  
 476  
 477  
 478  
 479  
 480  
 481  
 482  
 483  
 484  
 485  
 Figure 5: Analytical solution for the second velocity component

486  
487  
488  
489  
490  
491  
492  
493  
494  
495  
496  
497  
498  
499  
500  
501  
502  
503  
504  
505  
506  
507  
508  
509  
510  
511  
512  
513  
514  
515  
516  
517  
518  
519  
520  
521  
522  
523  
524  
525  
526  
527  
528  
529  
530  
531  
532  
533  
534  
535  
536  
537  
538  
539

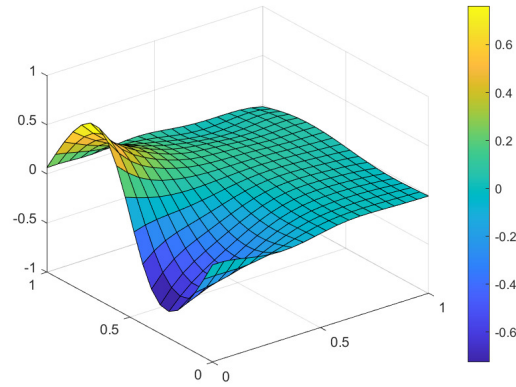


Figure 6: The second component of speed obtained as a result of network operation

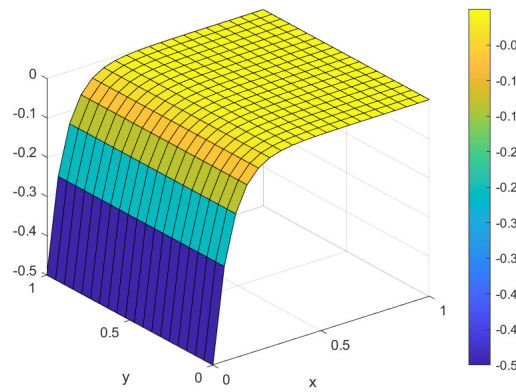


Figure 7: Analytical solution for pressure

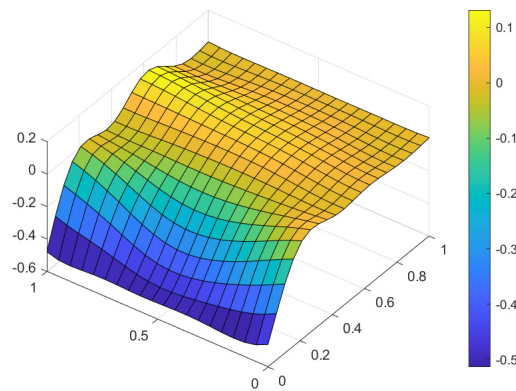
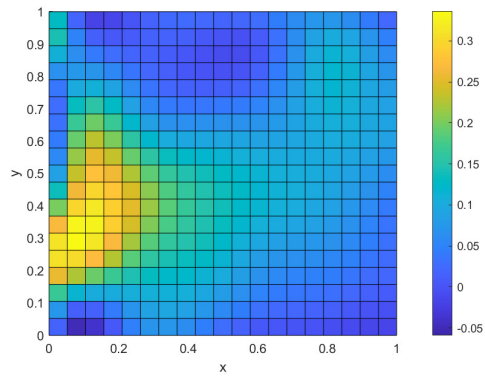
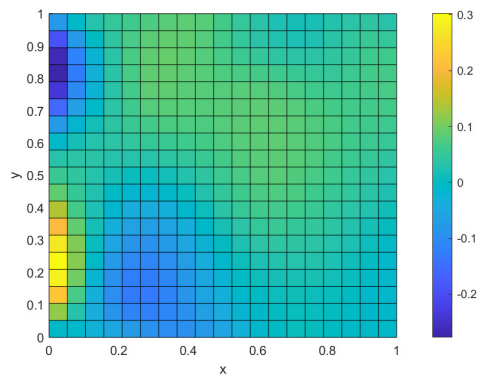


Figure 8: Pressure obtained as a result of network operation

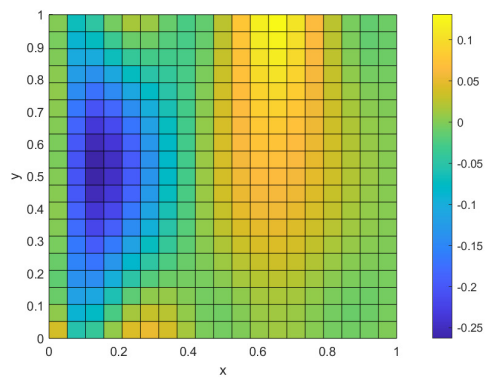
540 Error graphs compared with the analytical solution for the two components of velocity and pressure  
541 are shown in Figures 9, 10, 11.  
542  
543



544  
545  
546  
547  
548  
549  
550  
551  
552  
553  
554  
555  
556  
557 Figure 9: Error compared to the analytical solution for the first speed component



558  
559  
560  
561  
562  
563  
564  
565  
566  
567  
568  
569  
570  
571  
572  
573 Figure 10: Error compared to the analytical solution for the second speed component



574  
575  
576  
577  
578  
579  
580  
581  
582  
583  
584  
585  
586  
587  
588  
589  
590  
591  
592  
593  
594  
595  
596  
597  
598  
599  
600  
601  
602  
603  
604  
605  
606  
607  
608  
609  
610  
611  
612  
613  
614  
615  
616  
617  
618  
619  
620  
621  
622  
623  
624  
625  
626  
627  
628  
629  
630  
631  
632  
633  
634  
635  
636  
637  
638  
639  
640  
641  
642  
643  
644  
645  
646  
647  
648  
649  
650  
651  
652  
653  
654  
655  
656  
657  
658  
659  
660  
661  
662  
663  
664  
665  
666  
667  
668  
669  
670  
671  
672  
673  
674  
675  
676  
677  
678  
679  
680  
681  
682  
683  
684  
685  
686  
687  
688  
689  
690  
691  
692  
693  
694  
695  
696  
697  
698  
699  
700  
701  
702  
703  
704  
705  
706  
707  
708  
709  
710  
711  
712  
713  
714  
715  
716  
717  
718  
719  
720  
721  
722  
723  
724  
725  
726  
727  
728  
729  
730  
731  
732  
733  
734  
735  
736  
737  
738  
739  
740  
741  
742  
743  
744  
745  
746  
747  
748  
749  
750  
751  
752  
753  
754  
755  
756  
757  
758  
759  
760  
761  
762  
763  
764  
765  
766  
767  
768  
769  
770  
771  
772  
773  
774  
775  
776  
777  
778  
779  
780  
781  
782  
783  
784  
785  
786  
787  
788  
789  
790  
791  
792  
793  
794  
795  
796  
797  
798  
799  
800  
801  
802  
803  
804  
805  
806  
807  
808  
809  
810  
811  
812  
813  
814  
815  
816  
817  
818  
819  
820  
821  
822  
823  
824  
825  
826  
827  
828  
829  
830  
831  
832  
833  
834  
835  
836  
837  
838  
839  
840  
841  
842  
843  
844  
845  
846  
847  
848  
849  
850  
851  
852  
853  
854  
855  
856  
857  
858  
859  
860  
861  
862  
863  
864  
865  
866  
867  
868  
869  
870  
871  
872  
873  
874  
875  
876  
877  
878  
879  
880  
881  
882  
883  
884  
885  
886  
887  
888  
889  
890  
891  
892  
893  
894  
895  
896  
897  
898  
899  
900  
901  
902  
903  
904  
905  
906  
907  
908  
909  
910  
911  
912  
913  
914  
915  
916  
917  
918  
919  
920  
921  
922  
923  
924  
925  
926  
927  
928  
929  
930  
931  
932  
933  
934  
935  
936  
937  
938  
939  
940  
941  
942  
943  
944  
945  
946  
947  
948  
949  
950  
951  
952  
953  
954  
955  
956  
957  
958  
959  
960  
961  
962  
963  
964  
965  
966  
967  
968  
969  
970  
971  
972  
973  
974  
975  
976  
977  
978  
979  
980  
981  
982  
983  
984  
985  
986  
987  
988  
989  
990  
991  
992  
993  
994  
995  
996  
997  
998  
999  
1000

594 This problem was solved on a fully connected network (29). Physics-informed radial basis function  
 595 networks are as accurate as fully connected networks, but they are easier and faster to train.  
 596

## 597 4 CONCLUSION

598 Algorithms and programs for solving direct and inverse boundary value problems on physically in-  
 599 formed networks of radial basis functions have been developed. An algorithm and programs for  
 600 solving a system of differential equations for solving two-dimensional stationary Navier-Stokes  
 601 equations using networks of radial basis functions have been developed. The gradient descent  
 602 method, Nesterov’s method, Levenberg-Marquardt method, and Hessian diagonal approximation  
 603 method have been adapted to solve the problems. Further development of the work involves devel-  
 604 oping an extension for one of the neural network implementation libraries in order to implement  
 605 physically informed networks of radial basis functions using automatic differentiation. This will ex-  
 606 pand the possibilities of using physically informed networks of radial basis functions and will allow  
 607 objectively comparing physically informed neural networks of different architectures.  
 608

## 609 REFERENCES

- 610
- 611 [1] D.I.Fotiadis I.E.Lagaris, A.Likas. Artificial neural networks for solving ordinary and partial  
 612 differential equations. *IEEE Transactions on Neural Networks*, 9:987–1000, 1998.  
 613
- 614 [2] M. Kumar N. Yadav, A. Yadav. An introduction to neural network methods for differential  
 615 equations. *Dordrecht*, page 115, 2015.  
 616
- 617 [3] G. Cybenko. Approximation by superposition of a sigmoidal function. *mathematics of control.*  
 618 *Signals and Systems*, 2:303–314, 1989.  
 619
- 620 [4] K. Hornik. Approximation capabilities of multilayer feedforward networks. *NeuralNetworks*,  
 621 4(2):251–257, 1999.
- 622 [5] G.E. Karniadakis M. Raissi, P. Perdikaris. Physics-informed neural networks: A deep learning  
 623 framework for solving forward and inverse problems involving nonlinear partial differential  
 624 equations. *Journal of Computational Physics*, 378:686–707, 2019.  
 625
- 626 [6] Z. Mao G.E. Karniadakis L. Lu, X. Meng. Deepxde: A deep learning library for solving  
 627 differential equations. *SIAM Review*, 63(1):208–228, 2021.  
 628
- 629 [7] F. Giampaolo G. Rozza M. Raissi F. Francesco Piccialli S. Cuomo, V.S. Di Cola. Scientific  
 630 machine learning through physics–informed neural networks: Where we are and what’s next.  
 631 *Journal of Scientific Computing*, 92:88, 2022.
- 632 [8] P. Ramachandran A.A. Ramabathiran. Spinn: Sparse, physics-based, and partially interpretable  
 633 neural networks for pdes. *Journal of Computational Physics*, page 445, 2021.  
 634
- 635 [9] A. Wong A. Hryniewski. Deepplabnet: End-to-end learning of deep radial basis networks with  
 636 fully learnable basis functions.
- 637 [10] M.D. Buhmann. Radial basis functions: Theory and implementations. *Cambridge, Cambridge*  
 638 *University Pres*, page 259, 2004.  
 639
- 640 [11] G.E. Karniadakisa M. Raissi, P. Perdikaris. Physics-informed neural networks: A deep learning  
 641 framework for solving forward and inverse problems involving nonlinear partial differential  
 642 equations. *Journal of Computational Physics*, 378:686–707, 2019.
- 643 [12] D.A. Stenkin V.I. Gorbachenko. Solving equations describing processes in a piecewise ho-  
 644 mogeneous medium on radial basis functions networks. *Neuroinformatics 2020. Studies in*  
 645 *Computational Intelligence*, 1008:412–419, 2021.  
 646
- 647 [13] D.A. Stenkin V.I. Gorbachenko. Deep radial basis function networks. *7th International Con-*  
*ference on Contemporary Information Technology and Mathematics*, page 267–273, 2021.

- 648 [14] D.A. Stenkin V.I. Gorbachenko. Physics-informed radial basis function networks: Solving  
649 inverse problems for partial differential equations. *Cyber-Physical Systems and Control II.*  
650 *CPSC 2021. Lecture Notes in Networks and Systems*, 460:3–12, 2023.
- 651 [15] D.A. Stenkin V.I. Gorbachenko. Solving of inverse coefficient problems on networks of radial  
652 basis functions. *Advances in Neural Computation, Machine Learning, and Cognitive Research*  
653 *V. Neuroinformatics 2021*, 1008:230–237, 2022.
- 654 [16] D.A. Stenkin V.I. Gorbachenko. Physics-informed radial basis-function networks. *Technical*  
655 *Physics*, 68:151–157, 2023.
- 656 [17] D.A. Stenkin V.I. Gorbachenko. Mathematical modeling on a physics-informed radial basis  
657 function network. *Mathematics*, 12(2):241, 2024.
- 658 [18] A.N. Kolmogorov. On the representation of continuous functions of many variables by super-  
659 position of continuous functions of one variable and addition. *Russian Academy of Sciences*,  
660 114(5):953–956, 1957.
- 661 [19] Hecht-Nielsen R. Kolmogorov’s mapping neural network existence theorem. *IEEE First An-*  
662 *annual Int. Conf. on Neural Networks*, 3(2):11–13, 1987.
- 663 [20] Z. Liu Y. Wang S. Vaidya F. Ruehle J. Halverson M. Soljačić T.Y. Hou, M. Tegmark. Kan:  
664 Kolmogorov-arnold networks. <https://arxiv.org/abs/2404.19756>.
- 665 [21] Z. Li. Kolmogorov-arnold networks are radial basis function networks. <https://arxiv.org/abs/2405.06721>.
- 666 [22] S. Wright J. Nocedal. Numerical optimization. *Springer*, 378:2006, 2006.
- 667 [23] D.W. Marquardt. An algorithm for least-squares estimation of nonlinear parameters. *Journal*  
668 *of the Society for Industrial and Applied Mathematics*, 11:431–441, 1963.
- 669 [24] P.N. Vabishchevich A.A. Samarskii. Numerical methods for solving inverse problems of math-  
670 ematical physics. *Berlin: Walter de Gruyter*, 52:454, 2007.
- 671 [25] V.A. Morozov. Methods for solving incorrectly posed problems. *New York: Springer*, page  
672 280, 1984.
- 673 [26] L.S.G. Kovasznay. Laminar flow behind a two-dimensional grid. *Mathematical Proceedings*  
674 *of the Cambridge*, 44(1):58–62, 1948.
- 675 [27] N. A. Slezkin. *Dynamics of viscous incompressible fluid*. state publishing house of technical  
676 and theoretical literature, 1955.
- 677 [28] Y. E. Nesterov. Introduction to convex optimization. *Moscow Center for Continuous Mathe-*  
678 *matical Education*, page 280, 2010.
- 679 [29] S.V.Strizhak K.B.Koshelev. The use of a physically based neural network on the example  
680 of modeling hydrodynamic processes that allow an analytical solution. *Proceedings of the*  
681 *Institute of System Programming of the Russian Academy of Sciences*, 5:245–258, 2023.
- 682  
683  
684  
685  
686  
687  
688  
689  
690  
691  
692  
693  
694  
695  
696  
697  
698  
699  
700  
701